

Effective model approach to meson screening masses at finite temperature

Masahiro Ishii,^{1,*} Takahiro Sasaki,^{1,†} Kouji Kashiwa,^{2,‡} Hiroaki Kouno,^{3,§} and Masanobu Yahiro^{1,¶}

¹*Department of Physics, Graduate School of Sciences, Kyushu University, Fukuoka 812-8581, Japan*

²*RIKEN/BNL, Brookhaven, National Laboratory, Upton, New York 11973, USA*

³*Department of Physics, Saga University, Saga 840-8502, Japan*

(Dated: October 9, 2018)

Temperature dependence of pion and sigma-meson screening masses is evaluated by the Polyakov-loop extended Nambu–Jona-Lasinio (PNJL) model with the entanglement vertex. We propose a practical way of calculating meson screening masses in the NJL-type effective models. The method based on the Pauli-Villars regularization solves the well-known difficulty that the evaluation of screening masses is not easy in the NJL-type effective models. The PNJL model with the entanglement vertex and the Pauli-Villars regularization well reproduces lattice QCD results on temperature dependence of the chiral condensate and the Polyakov loop. The method is applied to analyze temperature dependence of pion screening masses calculated with state-of-the-art lattice simulations with success in reproducing the lattice QCD results.

PACS numbers: 11.30.Rd, 12.40.-y, 21.65.Qr, 25.75.Nq

I. INTRODUCTION

Meson masses are not only fundamental quantities of hadrons but also a key to know properties of quantum chromodynamics (QCD) vacuum. For example, temperature (T) dependence of pion and sigma-meson masses is strongly related to chiral symmetry restoration of QCD vacuum. Such light mesons play an important role in nuclear physics as mediators of the nuclear force. T dependence of light meson masses affects the equation of state particularly around and above the pseudocritical temperature T_c of chiral and deconfinement crossover temperature [1, 2].

Lattice QCD (LQCD) is the first-principle calculation of QCD. At finite T , meson pole (screening) masses are calculated from the exponential decay of temporal (spatial) mesonic correlation functions. LQCD simulations are more difficult for pole masses than for screening masses, since the lattice size is smaller in the time direction than in the spatial direction. This situation becomes more serious as T increases. For this reason, meson screening masses were calculated in most of the LQCD simulations. Recently, a state-of-the-art calculation was done for meson screening masses in a wide range of $T < 4T_c \approx 800$ MeV [3].

Constructing the effective model is an approach complementary to the first-principle LQCD simulation. For example, the phase structure and light meson pole masses are extensively investigated at finite T by the Nambu–Jona-Lasinio (NJL) model [4, 5] and the Polyakov-loop extended Nambu–Jona-Lasinio (PNJL) model [6–18]. The NJL model treats the chiral symmetry breaking, but not the confinement mechanism. Meanwhile, the PNJL model is designed [8] to treat the confinement mechanism approximately in addition to

the chiral symmetry breaking. In this sense, the PNJL model is superior to the NJL model. In the two-flavor PNJL model the chiral and deconfinement transitions do not coincide with each other when the model parameters are set to reproduce the realistic transition temperature [11], whereas the coincidence is seen in the two-flavor LQCD simulations. This problem is solved by introducing the four-quark vertex depending on the Polyakov loop [19, 20]. The model with the entangle vertex is called the entanglement-PNJL (EPNJL) model. The EPNJL model can also reproduce the QCD phase structure at imaginary chemical potential [21, 22] and at real isospin chemical potential [23] where LQCD is feasible.

The NJL-type effective models are quite practical. In fact, meson pole masses have been extensively studied with the models. However, only a few trials were made so far for the evaluation of meson screening masses $M_{\xi, \text{scr}}$ [24, 25]; here ξ means a species of mesons. The model calculations have essentially two problems. One problem is that the NJL-type models are nonrenormalizable and hence the regularization is needed in the model calculations. The regularization commonly used is the three-dimensional momentum cutoff. The momentum cutoff breaks Lorentz invariance and thereby the spatial correlation function $\eta_{\xi\xi}(r)$ has an unphysical oscillation [25]. This makes the determination of $M_{\xi, \text{scr}}$ quite difficult, since $M_{\xi, \text{scr}}$ is defined from the exponential decay of $\eta_{\xi\xi}(r)$ at large distance (r):

$$M_{\xi, \text{scr}} = - \lim_{r \rightarrow \infty} \frac{d \ln \eta_{\xi\xi}(r)}{dr}. \quad (1)$$

Another problem is the feasibility of numerical calculations. In the model approach, $\eta_{\xi\xi}(r)$ is first obtained in the momentum ($\tilde{q} = \pm|\mathbf{q}|$) representation $\chi_{\xi\xi}(0, \tilde{q}^2)$. In the Fourier transformation to the coordinate representation,

$$\eta_{\xi\xi}(r) = \frac{1}{4\pi^2 i r} \int_{-\infty}^{\infty} d\tilde{q} \tilde{q} \chi_{\xi\xi}(0, \tilde{q}^2) e^{i\tilde{q}r}, \quad (2)$$

the integrand is slowly damping and highly oscillating particularly at large r where $M_{\xi, \text{scr}}$ is defined. This requires heavy numerical calculations. It was then proposed that the contour

*ishii@phys.kyushu-u.ac.jp

†sasaki@phys.kyushu-u.ac.jp

‡kashiwa@ribf.riken.jp

§kounoh@cc.saga-u.ac.jp

¶yahiro@phys.kyushu-u.ac.jp

integral was made in the complex- \tilde{q} plane [25]. However, the contour integral is still hard to do because of the presence of the temperature cuts in the vicinity of the real axis [25]; see the left panel of Fig. 1, where note that ϵ is an infinitesimal quantity.

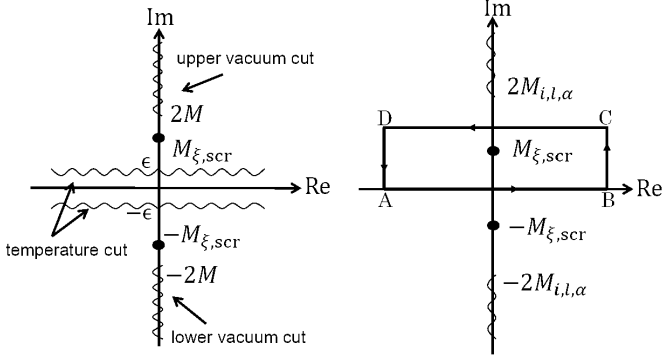


Fig. 1: Singularities of $\chi_{\xi\xi}(0, \tilde{q})$ in the complex- \tilde{q} plane based on the previous formulation [25] (left) and the present formulation (right). Cuts are denoted by the wavy lines and poles by the points.

In this paper, we propose a practical way of calculating $M_{\xi,scr}$ in the NJL-type effective models. The first problem is solved by using the Pauli-Villars (PV) regularization [25, 26] that preserves Lorentz symmetry. The EPNJL model with the PV regularization well reproduces two-flavor LQCD results on T dependence of the chiral condensate and the Polyakov loop. The second problem is solved by deriving a new expression for $\chi_{\xi\xi}(0, \tilde{q}^2)$. In the expression, the contributions of the vacuum and temperature cuts to $\eta_{\xi\xi}(r)$ are partially canceled in the complex- \tilde{q} plane. A pole is well isolated from the resultant cut; see the right panel of Fig. 1. The screening mass can therefore be obtained from the location of the pole without making the Fourier transform to the coordinate representation. The proposed method is applied to analyze T dependence of pion screening mass obtained by state-of-the-art 2+1 flavor LQCD simulations [3].

II. FORMALISM

We first recapitulate the EPNJL model [19, 20] and derive the equations for meson pole and screening masses from the Schwinger-Dyson equation for the quark-antiquark scattering.

The Lagrangian density of the two-flavor isospin symmetric EPNJL model is defined as

$$\mathcal{L} = \bar{q}(i\gamma_\nu D^\nu - m_0)q + G_s(\Phi)[(\bar{q}q)^2 + (\bar{q}i\gamma_5\vec{\tau}q)^2] - \mathcal{U}(\Phi[A], \bar{\Phi}[A], T) \quad (3)$$

with the quark field q , the current quark mass m_0 and the isospin matrix $\vec{\tau}$. The coupling constant $G_s(\Phi)$ of the four-quark interaction depends on the Polyakov loop Φ as

$$G_s(\Phi) = G_s [1 - \alpha_1 \Phi \bar{\Phi} - \alpha_2 (\Phi^3 + \bar{\Phi}^3)], \quad (4)$$

where $D^\nu = \partial^\nu + iA^\nu$ with $A^\nu = \delta_0^\nu g(A^0)_a \lambda_a / 2 = -\delta_0^\nu i g(A_4)_a \lambda_a / 2$ for the gauge field A_a^ν , the Gell-Mann matrix λ_a and the gauge coupling g . When $\alpha_1 = \alpha_2 = 0$, the EPNJL model is reduced to the PNJL model[6–18].

In the EPNJL model, only the time component of A_μ is treated as a homogeneous and static background field, which is governed by the Polyakov-loop potential \mathcal{U} . The Polyakov loop Φ and its conjugate $\bar{\Phi}$ are then obtained in the Polyakov gauge by

$$\Phi = \frac{1}{3} \text{tr}_c(L), \quad \bar{\Phi} = \frac{1}{3} \text{tr}_c(L^*) \quad (5)$$

with $L = \exp[iA_4/T] = \exp[i\text{diag}(A_4^{11}, A_4^{22}, A_4^{33})/T]$ for the classical variables A_4^{ii} satisfying that $A_4^{11} + A_4^{22} + A_4^{33} = 0$. In the determination of the A_4^{ii} from Φ and $\bar{\Phi}$, there is an arbitrariness coming from color symmetry. The arbitrariness does not change any physics. For zero chemical potential ($\mu = 0$), Φ equals to $\bar{\Phi}$. Hence it is possible to choose $A_4^{33} = 0$ and determine the others as $A_4^{22} = -A_4^{11} = \cos^{-1}(\frac{3\Phi-1}{2})T$.

We use the logarithm-type Polyakov-loop potential \mathcal{U} of Ref. [14]. The parameter set in \mathcal{U} is fitted to reproduce LQCD data at finite T in the pure gauge limit. The \mathcal{U} yields the first-order deconfinement phase transition at $T = T_0$. In the pure gauge limit, LQCD data show the phase transition at $T = 270$ MeV. Hence the parameter T_0 is often set to 270 MeV, but the EPNJL model with this value of T_0 yields a larger value of T_c for the deconfinement transition than the two-flavor LQCD prediction $T_c^{2f} \approx 173 \pm 8$ MeV [1, 27, 28]. This problem can be solved by rescaling T_0 . In fact, the EPNJL model with $T_0 = 200$ MeV and $\alpha_1 = \alpha_2 = 0.20$ reproduces the two-flavor-LQCD result.

Making the mean field approximation(MFA) to (3) leads to the linearized Lagrangian density

$$\mathcal{L}^{\text{MFA}} = \bar{q}S^{-1}q - G_s(\Phi)\sigma^2 - \mathcal{U}(\Phi[A], \bar{\Phi}[A], T) \quad (6)$$

with the quark propagator

$$S = \frac{1}{i\gamma_\nu \partial^\nu - i\gamma_0 A_4 - M} \quad (7)$$

with the effective quark mass $M = m_0 - 2G_s(\Phi)\sigma$. Making the path integral over the quark field, one can get the thermodynamic potential (per unit volume) as

$$\begin{aligned} \Omega_{\text{PNJL}} &= U_{\text{M}} + \mathcal{U} - 2N_f \int \frac{d^3p}{(2\pi)^3} \left[3E_p \right. \\ &+ \frac{1}{\beta} \ln [1 + 3(\Phi + \bar{\Phi}e^{-\beta(E_p-\mu)})e^{-\beta(E_p-\mu)} + e^{-3\beta(E_p-\mu)}] \\ &+ \left. \frac{1}{\beta} \ln [1 + 3(\bar{\Phi} + \Phi e^{-\beta(E_p+\mu)})e^{-\beta(E_p+\mu)} + e^{-3\beta(E_p+\mu)}] \right] \end{aligned} \quad (8)$$

with $\beta = 1/T$, $E_p = \sqrt{\mathbf{p}^2 + M^2}$ and $U_{\text{M}} = G_s(\Phi)\sigma^2$, where N_f is the number of flavors.

Since the momentum integral of (8) diverges, we use the PV regularization [25, 26]. In the scheme, the integral $I(M, q)$ is regularized as

$$I^{\text{reg}}(M, q) = \sum_{\alpha=0}^2 C_{\alpha} I(M_{\alpha}, q), \quad (9)$$

where $M_0 = M$ and M_{α} ($\alpha \geq 1$) are masses of auxiliary particles. The parameters M_{α} and C_{α} should satisfy the condition $\sum_{\alpha=0}^2 C_{\alpha} = \sum_{\alpha=0}^2 C_{\alpha} M_{\alpha}^2 = 0$. We then assume $(C_0, C_1, C_2) = (1, 1, -2)$ and $(M_1^2, M_2^2) = (M^2 + 2\Lambda^2, M^2 + \Lambda^2)$. We keep the parameter Λ finite even after the subtraction (9), since the present model is nonrenormalizable. The parameters taken are $m_0 = 6.3$ MeV, $G_s = 5.0$ GeV $^{-2}$ and $\Lambda = 0.768$ GeV. This parameter set reproduces the pion decay constant $f_{\pi} = 93.3$ MeV and the pion mass $M_{\pi} = 138$ MeV at vacuum.

We derive the equations for pion and sigma-meson masses, following Ref [15]. Now we consider the case of $\mu = 0$. The pseudoscalar isovector current with the same quantum number as pion is

$$J_P^a(x) = \bar{q}(x) i\gamma_5 \tau^a q(x) \quad (10)$$

and the scalar isoscalar current with the same quantum number as sigma meson is

$$J_S(x) = \bar{q}(x)q(x) - \langle \bar{q}(x)q(x) \rangle. \quad (11)$$

The Fourier transform of the mesonic correlation function $\chi_{\xi\xi}(x) \equiv \langle 0|T \left(J_{\xi}(x) J_{\xi}^{\dagger}(0) \right) |0 \rangle$ is

$$\chi_{\xi\xi}(q^2) = i \int d^4x e^{iq \cdot x} \langle 0|T \left(J_{\xi}(x) J_{\xi}^{\dagger}(0) \right) |0 \rangle, \quad (12)$$

where $\xi = P^a$ for pion and S for sigma meson and T stands for the time-ordered product. Since we deal with only pion and sigma meson, there is no mixing term $\chi_{\xi\xi'}$ ($\xi' \neq \xi$). Using the random-phase (ring) approximation, one can obtain the Schwinger-Dyson equation

$$\chi_{\xi\xi}(q^2) = \Pi_{\xi\xi}(q^2) + 2G_s(\Phi) \Pi_{\xi\xi}(q^2) \chi_{\xi\xi}(q^2) \quad (13)$$

for $\chi_{\xi\xi}(q^2)$, where the one-loop polarization function $\Pi_{\xi\xi}$ is defined as

$$\Pi_{\xi\xi} \equiv (-i) \int \frac{d^4p}{(2\pi)^4} \text{Tr} (G_{\xi} iS(p'+q) G_{\xi} iS(p')) \quad (14)$$

with $p' = (p_0 + iA_4, \mathbf{p})$, the quark propagator $S(q)$ in the Hartree approximation and $G_{\xi} = G_P^a = i\gamma_5 \tau^a$ for pion and $G_{\xi} = G_S = 1$ for sigma meson. The solution to (13) is

$$\chi_{\xi\xi} = \frac{\Pi_{\xi\xi}(q^2)}{1 - 2G_s(\Phi) \Pi_{\xi\xi}(q^2)}. \quad (15)$$

At $T = 0$, $\chi_{\xi\xi}$ and $\Pi_{\xi\xi}$ are functions of $q^2 = q_0^2 - \mathbf{q}^2$, but for later convenience we denote them as $\chi_{\xi\xi}(q_0^2, \mathbf{q}^2)$ and

$\Pi_{\xi\xi}(q_0^2, \mathbf{q}^2)$. For $T = 0$, $\Pi_{\xi\xi}$ is explicitly obtained by

$$\begin{aligned} \Pi_{SS} &= i \int \frac{d^4p}{(2\pi)^4} \text{Tr} \left[\frac{\{\gamma_{\mu}(p'+q)^{\mu} + M\} (\gamma_{\nu} p'^{\nu} + M)}{\{(p'+q)^2 - M^2\} (p'^2 - M^2)} \right] \\ &= 2iN_f [I_1 + I_2 - (q^2 - 4M^2)I_3], \end{aligned} \quad (16)$$

$$\begin{aligned} \Pi_{PP} &= i \int \frac{d^4p}{(2\pi)^4} \text{Tr} \left[(i\gamma_5 \tau^a) \frac{\{\gamma_{\mu}(p'+q)^{\mu} + M\}}{\{(p'+q)^2 - M^2\}} \right. \\ &\quad \left. \times (i\gamma_5 \tau^a) \frac{(\gamma_{\nu} p'^{\nu} + M)}{(p'^2 - M^2)} \right] \\ &= 2iN_f [I_1 + I_2 - q^2 I_3], \end{aligned} \quad (17)$$

with

$$I_1 = \int \frac{d^4p}{(2\pi)^4} \text{tr}_c \left[\frac{1}{p'^2 - M^2} \right], \quad (18)$$

$$I_2(q_0^2, \mathbf{q}^2) = \int \frac{d^4p}{(2\pi)^4} \text{tr}_c \left[\frac{1}{(p'+q)^2 - M^2} \right], \quad (19)$$

$$I_3(q_0^2, \mathbf{q}^2) = \int \frac{d^4p}{(2\pi)^4} \text{tr}_c \left[\frac{1}{\{(p'+q)^2 - M^2\} (p'^2 - M^2)} \right], \quad (20)$$

where tr_c means the trace of color matrix. For finite T , the corresponding equations are obtained by the replacement

$$\begin{aligned} p_0 &\rightarrow i\omega_l = i(2l+1)\pi T, \\ \int \frac{d^4p}{(2\pi)^4} &\rightarrow iT \sum_{l=-\infty}^{\infty} \int \frac{d^3p}{(2\pi)^3}. \end{aligned} \quad (21)$$

The meson pole mass M_{ξ} is a pole of $\chi_{\xi\xi}(q_0^2, \mathbf{q}^2)$. Taking the rest frame $q = (q_0, \mathbf{0})$ for convenience, one can get the equation for M_{ξ} as

$$[1 - 2G_{\xi\xi} \Pi_{\xi\xi}(q_0^2, 0)]|_{q_0=M_{\xi}} = 0. \quad (22)$$

The method of calculating meson pole masses is well established in the PNJL model [15].

The meson screening mass $M_{\xi, \text{scr}}$ defined with (1) is obtained by making the Fourier transform of $\chi_{\xi\xi}(0, \tilde{q}^2)$ as shown in (2). In the previous formalism [25], however, the procedure requires heavy numerical calculations in the I_3^{reg} part, as shown below, where I_3^{reg} means a function after the PV regularization. Taking the l summation before the p integral in (21), one can describe $I_3^{\text{reg}}(0, \tilde{q}^2)$ as the sum of the vacuum and temperature parts, $I_{3, \text{vac}}^{\text{reg}}$ and $I_{3, \text{tem}}^{\text{reg}}$, defined by

$$I_{3, \text{vac}}^{\text{reg}}(0, \tilde{q}^2) = \frac{-iN_c}{16\pi^2} \sum_{\alpha=0}^2 C_{\alpha} \left[\ln M_{\alpha}^2 + f_{\text{vac}} \left(\frac{2M_{\alpha}}{\tilde{q}} \right) \right], \quad (23)$$

$$f_{\text{vac}}(x) = \sqrt{1+x^2} \ln \left(\frac{\sqrt{1+x^2} + 1}{\sqrt{1+x^2} - 1} \right) \quad (24)$$

and

$$I_{3, \text{tem}}^{\text{reg}}(0, \tilde{q}^2) = \frac{iN_c}{16\pi^2} \sum_{\alpha=0}^2 C_{\alpha} \int_0^{\infty} d\tilde{p} f_{\text{tem}}(\tilde{p}, \tilde{q}) \left(F_{\tilde{p}}^{-} + F_{\tilde{p}}^{+} \right), \quad (25)$$

$$f_{\text{tem}}(\tilde{p}, \tilde{q}) = \frac{1}{E_{\tilde{p}} \tilde{q}} \ln \left(\frac{(\tilde{q} - 2\tilde{p})^2 + \epsilon^2}{(\tilde{q} + 2\tilde{p})^2 + \epsilon^2} \right), \quad (26)$$

where the Fermi distribution functions F_{\pm} are defined as

$$F_{\tilde{p}}^{\pm} = F^{\pm}(\tilde{p}, A_4, T) = \frac{1}{N_c} \sum_{i=1}^{N_c} \frac{1}{e^{(E_{\tilde{p}} \pm iA_4^i)/T} + 1}. \quad (27)$$

In (26), the ϵ^2 term is added to make the \tilde{p} integral well defined at $\tilde{q} = \pm 2\tilde{p}$, but this requires the limit of $\epsilon \rightarrow 0$.

As shown in the left panel of Fig. 1, $f_{\text{vac}}(2M_{\alpha}/\tilde{q})$ and $f_{\text{tem}}(\tilde{p}, \tilde{q})$ have the vacuum and temperature cuts in the complex \tilde{q} plane, respectively. In (2), the cuts contribute to the \tilde{q} integral in addition to the pole at $\tilde{q} = iM_{\xi, \text{scr}}$ defined by

$$[1 - 2G_{\xi\xi} \Pi_{\xi\xi}(0, \tilde{q}^2)]|_{\tilde{q}=iM_{\xi, \text{scr}}} = 0. \quad (28)$$

It is not easy to evaluate the temperature-cut contribution, since in (2) the integrand is slowly damping and highly oscillating with \tilde{q} near the real axis in the complex \tilde{q} plane. Furthermore we have to take the limit of $\epsilon \rightarrow 0$ finally.

A hint of solving this problem is in the high- T limit where $G_S = 0$. In this situation, it is known [25] that the vacuum- and temperature-cut contributions partially cancel each other. We then extend the discussion to general T . Using the formula

$$\frac{1}{e^x + 1} = \frac{1}{2} - \sum_{l=-\infty}^{\infty} \frac{x}{(2l+1)^2\pi^2 + x^2}, \quad (29)$$

we can rewrite $I_3^{\text{reg}}(0, \tilde{q})$ as

$$\begin{aligned} & I_{3, \text{tem}}^{\text{reg}}(0, \tilde{q}^2) \\ &= -I_{3, \text{vac}}^{\text{reg}}(0, \tilde{q}^2) + iT \sum_{i=1}^{N_c} \sum_{l=-\infty}^{\infty} \sum_{\alpha=0}^2 C_{\alpha} \\ &\times \int \frac{d^3p}{(2\pi)^3} \left[\frac{1}{\mathbf{p}^2 + M_{i, l, \alpha}^2} \frac{1}{(\mathbf{p} + \mathbf{q})^2 + M_{i, l, \alpha}^2} \right], \quad (30) \end{aligned}$$

where

$$M_{i, l, \alpha}(T) = \sqrt{M_{\alpha}^2 + \{(2l+1)\pi T + A_4^{ii}\}^2}. \quad (31)$$

Obviously, the first term in the right-hand side of (30) cancels $I_{3, \text{vac}}^{\text{reg}}$ in I_3^{reg} . To maintain this cancellation, we have to introduce the same regularization to both $I_{3, \text{tem}}^{\text{reg}}$ and $I_{3, \text{vac}}^{\text{reg}}$, although $I_{3, \text{tem}}$ is finite. Consequently we get

$$\begin{aligned} & I_3^{\text{reg}}(0, \tilde{q}^2) \\ &= \frac{iT}{2\pi^2} \sum_{i, l, \alpha} C_{\alpha} \int_0^1 dx \int_0^{\infty} d\tilde{k} \frac{\tilde{k}^2}{[\tilde{k}^2 + (x-x^2)\tilde{q}^2 + M_{i, l, \alpha}^2]^2} \\ &= \frac{iT}{4\pi\tilde{q}} \sum_{i, l, \alpha} C_{\alpha} \sin^{-1} \left(\frac{\tilde{q}}{\sqrt{\frac{\tilde{q}^2}{4} + M_{i, l, \alpha}^2}} \right). \quad (32) \end{aligned}$$

We have numerically checked that the convergence of l summation is quite fast in (32). Each term of $I_3^{\text{reg}}(0, \tilde{q})$ has only two cuts starting from $\pm 2iM_{i, l, \alpha}$ on the imaginary axis in the complex \tilde{q} plane. The cuts are shown in the right panel of Fig. 1. The lowest branch point is $\tilde{q} = 2iM_{i=1, l=0, \alpha=0}$.

Hence $2M_{i=1, l=0, \alpha=0}$ is regarded as ‘‘threshold mass’’ in the sense that the meson screening-mass spectrum becomes continuous above the point.

If $M_{\xi, \text{scr}} < 2M_{i=1, l=0, \alpha=0}$, the pole at $\tilde{q} = iM_{\xi, \text{scr}}$ is well isolated from the cut. Hence one can take the contour (A \rightarrow B \rightarrow C \rightarrow D \rightarrow A) shown in the right panel of Fig. 1. The \tilde{q} integral of $\tilde{q}\chi_{\xi\xi}(0, \tilde{q}^2)e^{i\tilde{q}r}$ on the real axis in (2) is then obtained from the residue at the pole and the line integral from point C to point D. The former behaves as $\exp[-M_{\xi, \text{scr}}r]/r$ at large r and the latter as $\exp[-2M_{i=1, l=0, \alpha=0}r]/r$. The behavior of $\eta_{\xi\xi}(r)$ at large r is thus determined by the pole. One can then determine the screening mass from the location of the pole in the complex- \tilde{q} plane without making the \tilde{q} integral. In the high- T limit, the condition tends to $M_{\xi, \text{scr}} < 2\pi T$.

III. NUMERICAL RESULTS

For T dependence of the chiral condensate σ and the Polyakov loop Φ in two-flavor LQCD simulations [29, 30], the EPNJL model with the PV regularization yields the same quality of agreement with the LQCD data as the model with the 3d-momentum cutoff regularization [20].

The pion screening mass $M_{\pi, \text{scr}}$ obtained by state-of-the-art 2+1 flavor LQCD simulations [3] is now analyzed by the present two-flavor EPNJL model simply, since the meson is composed of u and d quarks. This is a quantitative analysis, because the finite lattice-spacing effect is not negligible in the simulations. The chiral transition temperature evaluated is $T_c^{3f} = 196$ MeV in the simulations [3], although it becomes $T_c^{3f} = 154 \pm 9$ MeV in finer 2+1-flavor LQCD simulations [2] close to the continuum limit. Therefore, we rescale the LQCD results of Ref. [3] with multiplying them by the factor $154/196$ to reproduce $T_c^{3f} = 154 \pm 9$ MeV. The model parameters, m_0 and T_0 , are refitted to reproduce the rescaled 2+1 flavor LQCD data, i.e., $M_{\pi} = 175$ MeV at vacuum and $T_c^{3f} = 154 \pm 9$ MeV; the resulting values are $m_0 = 10.3$ MeV and $T_0 = 156$ MeV. The variation of m_0 from the original value 6.3 to 10.3 MeV little changes σ and Φ .

As shown in Fig. 2, the $M_{\pi, \text{scr}}$ calculated with the EPNJL model (solid line) well reproduces the LQCD result (open circles), when $\alpha_1 = \alpha_2 = 0.31$. In the PNJL model with $\alpha_1 = \alpha_2 = 0$, the model result (dotted line) largely underestimates the LQCD result, indicating that the entanglement is important. The dashed line denotes the sigma-meson screening mass $M_{\sigma, \text{scr}}$ obtained by the EPNJL model with $\alpha_1 = \alpha_2 = 0.31$. The solid and dashed lines are lower than the threshold mass $2M_{i=1, l=0, \alpha=0}$ (dot-dashed line). This guarantees that the $M_{\pi, \text{scr}}$ and $M_{\sigma, \text{scr}}$ determined from the location of the single pole in the complex- \tilde{q} plane agree with those from the exponential decay of $\eta_{\xi\xi}(r)$ at large r . The chiral restoration takes place at $T = T_c = 154$ MeV, since $M_{\pi, \text{scr}} = M_{\sigma, \text{scr}}$ there. After the restoration, the screening masses rapidly approach the threshold mass and finally $2\pi T$. The threshold mass is thus an important concept to understand T dependence of screening masses.

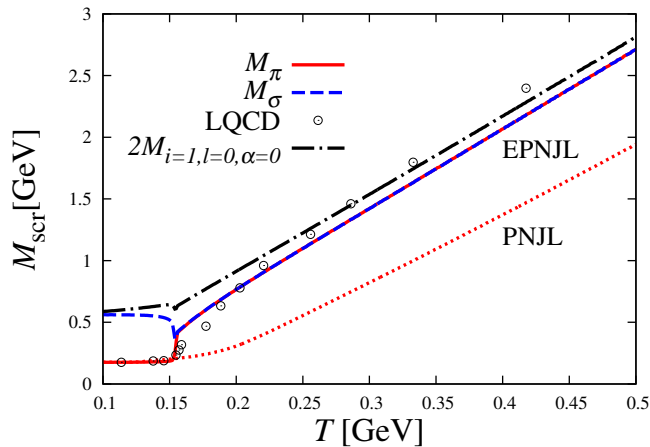


Fig. 2: T dependence of pion and sigma-meson screening masses, $M_{\pi,\text{scr}}$ and $M_{\sigma,\text{scr}}$. The solid and dashed lines denote $M_{\pi,\text{scr}}$ and $M_{\sigma,\text{scr}}$ calculated by the EPNJL model with $\alpha_1 = \alpha_2 = 0.31$, respectively, whereas the dotted line corresponds to $M_{\pi,\text{scr}}$ calculated with the PNJL model with $\alpha_1 = \alpha_2 = 0$. The open circles show $M_{\pi,\text{scr}}$ obtained by 2+1 flavor LQCD simulations [3]. The dot-dashed line stands for the threshold mass.

IV. SUMMARY

We have proposed a practical way of calculating meson screening masses $M_{\xi,\text{scr}}$ in the NJL-type models. This method based on the PV regularization solves the well-known difficulty that the evaluation of $M_{\xi,\text{scr}}$ is not easy in the NJL-type effective models. In the previous formalism [25], the vacuum and temperature cuts appear in the complex- \tilde{q} plane. The contributions to the mesonic correlation function are partially canceled in the present formalism. The branch point of the resultant cut can be regarded as the threshold mass. The pion and sigma-meson screening masses rapidly approach the threshold mass $2M_{i=1,l=0,\alpha=0}(T)$ after the chiral restoration.

Acknowledgments

The authors thank J. Takahashi for useful discussion. T.S. is supported by JSPS KAKENHI Grant No. 23-2790. K.K. is supported by RIKEN Special Postdoctoral Researchers Program.

-
- [1] Y. Aoki, G. Endrődi, A. Fodor, S. D. Katz, and K. K. Szabó, *Nature(London)* **443**, 675 (2006); S. Borsányi, Z. Fodor, C. Hoelbling, S. D. Katz, S. Krieg, C. Ratti, and K. K. Szabó, *J. High energy Phys.* 09 (2010) 073.
- [2] A. Bazavov *et al.*, *Phys. Rev. D* **80**, 014504 (2009); A. Bazavov *et al.*, *Phys. Rev. D* **85**, 054503 (2012);
- [3] M. Cheng, S. Datta, A. Francis, J. van der Heide, C. Jung, O. Kaczmarek, F. Karsch and E. Laermann *et al.*, *Eur. Phys. J. C* **71**, 1564 (2011).
- [4] Y. Nambu and G. Jona-Lasinio, *Phys. Rev.* **122**, 345 (1961); **124**, 246 (1961).
- [5] S. P. Klevansky *Rev. Mod. Phys.* **64**, 649 (1992); T. Hatsuda and T. Kunihiro *Phys. Rep.* **247**, 221 (1994); M. Buballa *Phys. Rep.* **407**, 205 (2005).
- [6] P. N. Meisinger, and M. C. Ogilvie, *Phys. Lett. B* **379**, 163 (1996).
- [7] A. Dumitru, and R. D. Pisarski, *Phys. Rev. D* **66**, 096003 (2002).
- [8] K. Fukushima, *Phys. Lett. B* **591**, 277 (2004); *Phys. Rev. D* **77**, 114028 (2008); **78**, 114019 (2008).
- [9] S. K. Ghosh, T. K. Mukherjee, M. G. Mustafa, and R. Ray, *Phys. Rev. D* **73**, 114007 (2006).
- [10] E. Megias, E. R. Arriola, and L. L. Salcedo, *Phys. Rev. D* **74**, 065005 (2006).
- [11] C. Ratti, M. A. Thaler, and W. Weise, *Phys. Rev. D* **73**, 014019 (2006).
- [12] M. Ciminale, R. Gatto, G. Nardulli, and M. Ruggieri, *Phys. Lett. B* **657**, 64 (2007); M. Ciminale, R. Gatto, N. D. Ippolito, G. Nardulli, and M. Ruggieri, *Phys. Rev. D* **77**, 054023 (2008).
- [13] C. Ratti, S. Rößner, M. A. Thaler, and W. Weise, *Eur. Phys. J. C* **49**, 213 (2007).
- [14] S. Rößner, C. Ratti, and W. Weise, *Phys. Rev. D* **75**, 034007 (2007).
- [15] H. Hansen, W. M. Alberico, A. Beraudo, A. Molinari, M. Nardi, and C. Ratti, *Phys. Rev. D* **75**, 065004 (2007).
- [16] C. Sasaki, B. Friman, and K. Redlich, *Phys. Rev. D* **75**, 074013 (2007).
- [17] B. -J. Schaefer, J. M. Pawłowski, and J. Wambach, *Phys. Rev. D* **76**, 074023 (2007).
- [18] K. Kashiwa, H. Kouno, M. Matsuzaki, and M. Yahiro, *Phys. Lett. B* **662**, 26 (2008).
- [19] Y. Sakai, T. Sasaki, H. Kouno, and M. Yahiro, *Phys. Rev. D* **82**, 076003 (2010).
- [20] T. Sasaki, Y. Sakai, H. Kouno, and M. Yahiro, *Phys. Rev. D* **84**, 091901 (2011).
- [21] M. D'Elia and F. Sanfilippo, *Phys. Rev. D* **80**, 111501 (2009).
- [22] P. de Forcrand and O. Philipsen, *Phys. Rev. Lett.* **105**, 152001 (2010).
- [23] J. B. Kogut and D. K. Sinclair, *Phys. Rev. D* **70**, 094501(2004).
- [24] T. Kunihiro, *Nucl. Phys. B* **351**, 593 (1991).
- [25] W. Florkowski, *Acta. Phys. Pol. B* **28**, 2079 (1997).
- [26] W. Pauli, and F. Villars, *Rev. Mod. Phys.* **21**, 434 (1949).
- [27] W. Söldner, *Proc. Sci., LATTICE2010* (2010) 215 [arXiv:1012.4484].
- [28] K. Kanaya, *AIP Conf. Proc.* **1343**, 57 (2011); *Proc. Sci., LATTICE2010* (2010) 01.
- [29] F. Karsch, *Lect. Notes Phys.* **583**, 209 (2002).
- [30] O. Kaczmarek and F. Zantow, *Phys. Rev. D* **71**, 114510 (2005).